Available online at www.sciencedirect.com
ScienceDirect
Scripta Materialia 62 (2010) 71–74
Scripta MATERIALIA
www.elsevier.com/locate/scriptamat

Microstructures and shape memory characteristics of a Ti–20Ni–30Cu (at.%) alloy strip fabricated by the melt overflow process

Seok-won Kang,[a] Yeon-Min Lim,[a] Yong-hee Lee,[a] Hyo-jung Moon,[a] Yeon-wook Kim[b] and Tae-hyun Nam[a,*]

[a]*School of Materials Science and Engineering & ERI, Gyeongsang National University, 900 Gazwadong, Jinju, Gyeongnam 660-701, Republic of Korea*

[b]*Department of Material Engineering, Keimyung University, 1000 Shindang-dong, Dalseo-gu, Taegu 704-710, Republic of Korea*

Received 17 August 2009; revised 7 September 2009; accepted 24 September 2009
Available online 27 September 2009

Melt overflow improved the workability and shape memory characteristics of a Ti–20Ni–30Cu (at.%) alloy by suppressing the formation of TiCu phase and introducing crystallographic defects such as dislocations. The fracture stress and strain of the alloy strip prepared by melt overflow were 445 MPa and 7.6%, respectively, which were larger than those of the alloy rod fabricated by conventional casting. Transformation hysteresis of the strip was 3.8 K under 120 MPa, which was much smaller than that of the rod.

Keywords: Shape memory alloys; Rapid solidification; Microstructure; Martensitic phase transformation; Transformation hysteresis

The B2 (cubic) → B19 (orthorhombic) martensitic transformation is known to be very suitable for actuators because of its large transformation elongation and small hysteresis [1]. The B2 → B19 transformation has been observed in Ti–Ni–Cu, Ti–Ni–Pd and Ti–Ni–Au alloys, which were made by substituting Cu, Pd and Au, respectively, for Ni in an equiatomic Ti–Ni binary alloy [2–4]. Of these additions, Cu is the most attractive from an economic point of view. The B2 → B19 transformation is observed in Ti–Ni–Cu alloys whose content is more than 10 at.% [2,5]. Unfortunately, Ti–Ni–Cu alloys with Cu content higher than 10 at.% are brittle, and therefore cannot be deformed into a wire or plate, which is necessary for fabricating actuators. Some studies have investigated new shape memory alloys that show the B2 → B19 transformation while keeping their ductility. Substitution of Fe or Mo for Ni in a Ti–45Ni–5Cu (at.%) alloy induces the B2 → B19 transformation and leads to good ductility [6,7].

Transformation hysteresis accompanied by the B2 → B19 transformation in Ti–Ni–Cu alloys decreases with increasing Cu content due to a decrease in lattice deformation [5]. Therefore, Ti–Ni–Cu alloys with high Cu content are desirable for actuators that operate sensitively according to a temperature change. In order to overcome the brittleness of the alloys, many metallurgical processing technologies have been examined, including powder metallurgy and rapid solidification, since both hot and cold working are not available for them [8–12]. The melt overflow process could be an alternative for fabricating Ti–Ni–Cu alloys with high Cu content because it enables strips to be obtained directly from the molten metal. In melt overflow, molten metal overflows from a reservoir onto the surface of a rotating chill block. Unlike melt spinning techniques, the melt stream is not extruded through an orifice to contact the chill block; rather, the melt pool simply overflows to contact the rotating chill surface. It was shown in a previous study [13] that Ti–Ni and Ti–Ni–Cu alloy strips show an excellent shape memory effect, originating from the refined grain and texture. To the best of our knowledge, however, the melt overflow process has not been applied to a Ti–20Ni–30Cu (at.%) alloy which exceeds the solubility limit of Cu [14]. Therefore, in this study, a Ti–20Ni–30Cu (at.%) alloy strip was prepared by the melt overflow process. The microstructure and shape memory characteristics of the strip were investigated, and then compared with those prepared by conventional casting.

A rod-type Ti–20Ni–30Cu alloy ingot was prepared by arc melting in a water-cooled Cu hearth, then poured

* Corresponding author. E-mail: tahynam@gsnu.ac.kr

1359-6462/$ - see front matter © 2009 Acta Materialia Inc. Published by Elsevier Ltd. All rights reserved.
doi:10.1016/j.scriptamat.2009.09.034

into a tube-type mold by vacuum injection. The alloy was remelted five times under a high-purity Ar atmosphere to ensure homogeneity before pouring. A part of the rod was used for fabricating a strip by melt overflow. It was placed in a water-cooled hearth and skull melted under an Ar atmosphere by a plasma beam, then the hearth was tilted about a rotating quenching wheel made of Mo. The linear speed of the wheel was kept at 0.51 m s^{-1}. From the melt overflow, a strip with 10 mm width and about 530 μm thickness was obtained. A part of the rod was homogenized at 1273 K for 36 ks under an Ar atmosphere, then solution treated at 1123 K for 3.6 ks in vacuum.

Samples for differential scanning calorimetry (DSC), X-ray diffraction (XRD), scanning electron microscopy (SEM), energy-dispersive spectroscopy (EDS), tensile tests and thermal cycling tests under constant load were cut from the strip and rod. They were mechanically polished with emery papers followed by electropolishing with an electrolyte which consists of 95 vol.% CH_3COOH and 5 vol.% $HClO_4$. In order to investigate transformation temperatures, DSC measurements with a cooling and heating rate of 0.17 K s^{-1} were made. X-ray diffraction was made using Cu K_α with a scan speed of 1° min^{-1}. Thermal cycling tests under the applied stress of 120 MPa with a cooling and heating rate of 0.017 K s^{-1} were made for investigating the shape memory effect. Tensile tests were made at room temperature and strain rate was 10^{-3} s^{-1}. The strain was measured using an extensometer.

Figure 1(a and b) shows SEM micrographs of the rod and strip of a Ti–20Ni–30Cu alloy, respectively. The second phase particles with block shape and needle shape are observed in the rod (Fig. 1a) as designated by A and B, respectively, while they are not observed in the strip (Fig. 1b). From the EDS, both A and B are found to be composed of 50.3 ± 0.6 at.% Ti, 47.2 ± 0.8 at.% Cu and 2.8 ± 0.5 at.% Ni. Most of the A and B are observed near grain boundaries. Figure 1(c and d) are XRD patterns corresponding to Figure 1(a and b), respectively. In Figure 1(c and d), "O", "C" and "T" indicate the B19 martensite, B2 parent phase and TiCu phase, respectively. The diffraction peaks corresponding to the B19 martensite and TiCu phase are found in the pattern of the rod, while those of the B2 and the B19 martensite are found in the strip. Therefore, the second particles observed in Figure 1(a) are known to be TiCu with a few atomic percent Ni. Composition of the matrix designated by C was found to be very close to the nominal composition, Ti–20Ni–30Cu. TiCu particles are formed because the Ti–20Ni–30Cu alloy exceeds the solubility limit of Cu (~25 at.%) [14]. However, despite exceeding the solubility limit of Cu, TiCu particles are not found in the strip. The high solidification rate in the melt overflow is considered to suppress the formation of TiCu particles.

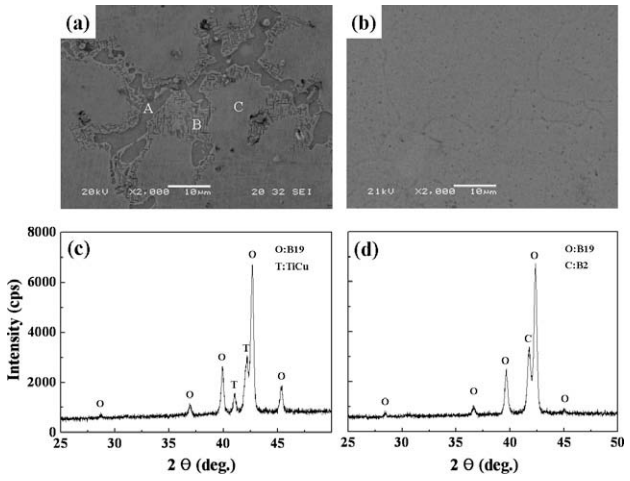

Figure 1. SEM photographs of a Ti–20Ni–30Cu alloy rod (a) and strip (b). The XRD patterns of (c) and (d) were obtained from the specimens of (a) and (b), respectively.

DSC curves of the rod and strip of a Ti–20Ni–30Cu alloy are shown in Figure 2(a and b), respectively. Clear DSC peaks are found on cooling and heating curves in both samples. From Figure 1(c and d), they are known to be due to the B2 → B19 transformation. It is found that the M_s (the B2 → B19 transformation start temperature) of the strip is 331 K, which is lower than that of the rod (341 K). TiCu particles are not believed to make the M_s of the rod higher than that of the strip because they are only formed near grain boundaries, as already mentioned. The chemical composition of the matrix is very close to the nominal composition, Ti–20Ni–30Cu (e.g. point C in Fig. 1a), which means that the chemical composition of the matrix is hardly changed by the formation of the TiCu phase. The matrix near the TiCu particles is expected to be Ti-poor when compared with the matrix far from the particles, which would decrease the M_s. Crystallographic defects, such as dislocation introduced by rapid solidification, are considered to be main reason for the lowering of the M_s of the strip, as reported by previous studies [15,16]. From Figure 2, the heat of transformation associated with the B2 → B19 in the rod is measured to be 17.6 J g^{-1}, which is slightly smaller than that of the strip (19.1 J g^{-1}). It is also found that the width of the DSC peaks of the strip is larger than that of the rod. Crystallographic defects, such as dislocation introduced by rapid solidification, are also considered to widen the DSC peaks of the strip.

Stress–strain curves of the rod and strip of a Ti–20Ni–30Cu alloy obtained from tensile tests at room temperature are shown in Figure 3(a and b), respectively. The stress plateau at about 50 MPa, designated by arrows in Figure 3(a), is attributed to the rearrangement of the B19 martensite variants since the matrix is in a fully martensitic state. On further loading, the specimen becomes elongated while keeping a linear relationship between stress and strain due to elastic deformation

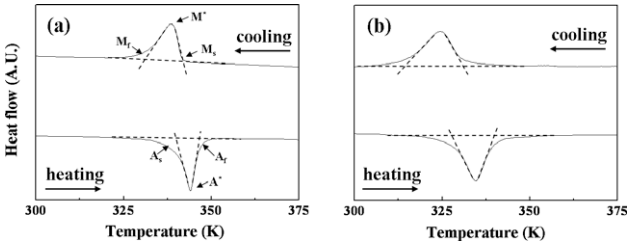

Figure 2. DSC curves of a Ti–20Ni–30Cu alloy rod (a) and strip (b).